Applied and Computational Mathematics
2014; 3(5): 197-204
Published online September 20, 2014 (http://www.sciencepublishinggroup.com/j/acm)
doi: 10.11648/j.acm.20140305.12
ISSN: 2328-5605 (Print); ISSN: 2328-5613 (Online)

Realization of inhomogeneous boundary conditions as virtual sources in parabolic and hyperbolic dynamics

Boe-Shong Hong

Department of Mechanical Engineering, National Chung Cheng University, Chia-Yi 62012, Taiwan

Email address:
imehbs@ccu.edu.tw

To cite this article:
Boe-Shong Hong. Realization of Inhomogeneous Boundary Conditions as Virtual Sources in Parabolic and Hyperbolic Dynamics. *Applied and Computational Mathematics.* Vol. 3, No. 5, 2014, pp. 197-204. doi: 10.11648/j.acm.20140305.12

Abstract: Scientists and engineers encounter many kinds of parabolic or hyperbolic distributed dynamics, which are often with inhomogeneous boundary conditions in practice. Boundary inhomogeneity makes the dynamics essentially nonlinear, which prevents the Hilbert space from being applied for modal decomposition and intelligent computation. Thus, this paper systematically deals with this situation via the conversion of the boundary inhomogeneity to a virtual source in conjunction with boundary homogeneity. For such a purpose, the 2D transfer-function is developed based on the Laplace-Galerkin integral transform as the main tool of this conversion. A section of numerical visualization is included to explore the topology of the virtual-source solution. Some interesting findings therein will be addressed.

Keywords: Inhomogeneous Boundary Conditions, nD Transfer Function Models, Robin Boundary Conditions, Sturm-Liouville Systems

1. Introduction

Civilization has encountered a great quantity of parabolic or hyperbolic dynamics in bounded domains- parabolic heat-conduction, acoustic wave, structure vibration, quantum mechanics, electromagnetic wave, hyperbolic heat-conduction, thermoacoustic oscillation, and so on. The partial differential equation governing any kind of these dynamics includes a spatially Laplacian operator or its higher orders, which is often spatially non-uniform. As the boundary condition, Dirichlet, von-Neumann, or Robin, of the Laplacian operator is homogeneous, its eigenfunctions constitute an admissible, real, orthogonal and complete basis in the Hilbert space of the operation domain. This basis provides modal decomposition of the dynamics for design purposes and computational intelligence. In many occasions, the boundary conditions are inhomogeneous; for instance, the heat-conduction constrained by environmental temperature is of inhomogeneous boundary condition, since temperature is non-zero in nature. With boundary inhomogeneity, the dynamics is essentially nonlinear, which prevents Hilbert space from being directly introduced for modal decomposition. With this paper, we will remedy this situation.

With the help of the Laplace-Galerkin integral transform in [1] and its inverse thereof, the inhomogeneous boundary conditions can be converted into virtual sources in conjunction with homogeneous boundary conditions. In closed form, such a source will be a Dirac Delta distribution or its spatial derivatives as a pointed input to the boundary, dubbed *boundary source*. This approach has ever been applied to identify thermal inertia in [2], and to derive the mechanical energy of thermoacoustics in [3]. In these decades, von-Neumann boundary source was employed to obtain order-reduced modelling of combustion instabilities in rocket motors [4-5]. Following these hints, this paper furthers the extension to Robin sources and explores the topological occurrence on boundary. Such an exploration counts mostly on the concept of *2D transfer-function*, wherein, with the Laplace-Galerkin transform, both equations governing the interior and the boundary are integrated into a single transfer function of two independent variables: one is from the time and the other is from the space. Performing the inverse Laplace-Galerkin transform of the 2D transfer-function realizes back the dynamics into homogeneous boundary conditions with boundary sources, both of which yield the identical solution in the interior. With boundary homogeneity, the elegant properties of Hilbert space are preserved to facilitate analyses.

The study on Robin inhomogeneity is fascinating and necessary for real practice, wherein the Dirichlet or von-Neumann boundary is considered as a simplified version of Robin boundary [6-9]. Therein, the boundary is the complement of the union of the exterior and the interior of the domain under consideration, so boundary conditions rely on the interaction between the process and the environment. Although such degenerative Robin helps escape many difficulties in numerical investigation, the actual Robin boundary should be identified through measured data for modern days of practice, as seen in [10-15] for examples. Therein, Robin boundaries are identified for the study of cancer destruction during hyperthermia treatment, the optical path length in inhomogeneous tissue, and axisymmetrical induction in heating processes, respectively. To be sure, the conversion of Robin inhomogeneity into boundary source can help make these important kinds of identification more accurate and reliable, since the realization of virtual source in principle suggests installing an active source into measurement to trig out desired data.

Virtual-source realization of boundary inhomogeneity also helps computational intelligence, addressed below. In cases of time-invariant environments, the response is usually computed by shifting the origin of spatial coordinate to the steady-state response, upon which the dynamics with homogeneous boundary condition can be solved by Separation of Variables [16]. This method can also be extended to time-varying environments by stepwise sampling the temporal continuity as in [17-18] for examples. Compared with the virtual-source solution, this solution is numerically tedious and incapable of capturing sudden changes in the environment. More importantly, the virtual-source conversion leads to input-output modelling that can be programmed into DSP microcontrollers for online signal processing.

Summarily, the virtual-source conversion of boundary inhomogeneity provides the following advantages that are beyond conventional approaches:

(1) Even with temporally discontinuous or impulsive environments, exact solutions can be calculated offline with the virtual-source realization.
(2) Modal decomposition is applicable for computational intelligence and order-reduced modelling.
(3) Active sources on boundary can be installed for identification of Robin coefficients.
(4) An overall distributed dynamics can be properly represented as feedback interconnection of sub-systems especially for impedance-matching design [3].
(5) As the control actuation is set on some boundary, the virtual-source realization generates a model served for feedback synthesis.
(6) It makes possible to apply the well-established digital signal processing (DSP) for online temporally varying environments.
(7) With the extended Kalman filtering, the environmental changes can be online estimated from the response of the dynamics, toward a newly sensing technology.

2. Mathematical Prerequisites

Consider a Laplacian operator A on spatial functions of a bounded region $\Omega \subset \Re^3$. The operator A is belonging to the Sturm-Liouville class [19] if its eigenfunctions constitute a real, orthonormal, and complete basis of $L_2(\Omega)$ under some inner-product $\langle \cdot,\cdot \rangle_\Omega$. We often distinguish a Sturm-Liouville operator by its self-adjointness and the compactness of its inverse. In the followings we give two examples often encountered in mechanical engineering.

Consider the elastic stiffness A:

$$\mathrm{A}\phi = -(1/\rho)\nabla\cdot(k\nabla\phi) \text{ in } \Omega,$$

$$\alpha\phi + \beta\nabla\phi\cdot\hat{n} = 0 \text{ on } \partial\Omega,$$

where $\rho(x) > 0$ and $k(x) > 0$ for $\forall x \in \Omega$ as well as $\alpha(x)$ and $\beta(x)$ are real but not both zero for $\forall x \in \partial\Omega$. Then the elastic stiffness belongs to Sturm-Liouville class, $\mathrm{A} \in \mathrm{SL}(\Omega)$, under the inner-product:

$$\langle \psi,\phi \rangle = \int_\Omega \rho(x)\phi^*(x)\psi(x)dV. \quad (1)$$

The proof of this claim follows.

Let $\psi,\varphi \in \mathrm{D(A)}$, that is,

$$\begin{bmatrix} \psi & \nabla\psi\cdot\hat{n} \\ \phi^* & \nabla\phi^*\cdot\hat{n} \end{bmatrix}\begin{bmatrix} \alpha \\ \beta \end{bmatrix} = 0 \text{ on } \partial\Omega,$$

which implies $\psi\nabla\phi^*\cdot\hat{n} - \phi^*\nabla\psi\cdot\hat{n} = 0$ on $\partial\Omega$ for any $\psi,\phi \in D(\mathrm{A})$, since $(\alpha,\beta) \neq (0,0)$. Then, based on the Green's second identity,

$$\begin{aligned} &\langle \mathrm{A}\psi,\phi \rangle - \langle \psi,\mathrm{A}\phi \rangle \\ &= \int_\Omega -\phi^*\nabla\cdot(k\nabla\psi) + \psi\nabla\cdot(k\nabla\phi^*)dV, \\ &= \oint_{\partial\Omega} k(-\phi^*\nabla\psi + \psi\nabla\phi^*)\cdot\hat{n}dS = 0 \end{aligned}$$

so $\langle \mathrm{A}\psi,\varphi \rangle = \langle \psi,\mathrm{A}\varphi \rangle$, i.e. A is self-adjoint. Denote by Λ the set of eigenvalues of A, with the corresponding eigenfunctions set $\Phi \equiv \{\varphi_\lambda \in \mathrm{D(A)}\}_{\lambda\in\Lambda}$, i.e.

$$\mathrm{A}\phi_\lambda = \lambda\phi_\lambda \text{ in } \Omega, \ \alpha\phi_\lambda + \beta\nabla\phi_\lambda\cdot\hat{n} = 0 \text{ on } \partial\Omega.$$

Firstly, with A's self-adjointness,

$$\begin{aligned} 0 &= \langle \mathrm{A}\phi_\lambda,\phi_\lambda \rangle - \langle \phi_\lambda,\mathrm{A}\phi_\lambda \rangle = \langle \lambda\phi_\lambda,\phi_\lambda \rangle - \langle \phi_\lambda,\lambda\phi_\lambda \rangle \\ &= (\lambda - \bar{\lambda})\langle \phi_\lambda,\phi_\lambda \rangle \end{aligned},$$

which implies $\lambda = \bar{\lambda}$, i.e. $\forall\lambda \in \Lambda$ are real. Thereby, the set of eigenfunctions Φ is also real. Moreover,

$$0 = \langle \mathrm{A}\phi_\lambda,\phi_\mu \rangle - \langle \phi_\lambda,\mathrm{A}\phi_\mu \rangle = (\lambda-\mu)\langle \phi_\lambda,\phi_\mu \rangle,$$

and thereby $\langle \phi_\lambda, \phi_\mu \rangle = 0$ for $\lambda \neq \mu$. That is, the set of eigenfunctions Φ is orthonormal if $\langle \phi_\lambda, \phi_\lambda \rangle$ is normalized to one for $\forall \lambda \in \Lambda$. Secondly, the inverse of A is a bounded and closed operator in $L_2(\Omega)$, since A is a second-order differential operator. Therefore, the set of eigenfunctions Φ is a complete basis of $L_2(\Omega)$.

Further to consider the bending stiffness A:

$$\mathsf{A}\phi = (1/\rho)\nabla^2(k\nabla^2\phi) \text{ in } \Omega,$$

$$\alpha_1\phi + \beta_1\nabla\phi\cdot\hat{n} = 0 \text{ and}$$

$$\alpha_2 k\nabla^2\phi + \beta_2\nabla(k\nabla^2\phi)\cdot\hat{n} = 0 \text{ on } \partial\Omega,$$

where the spatial functions ρ, k are real and positive in Ω, and $(\alpha_1,\beta_1)\neq(0.0)$, $(\alpha_2,\beta_2)\neq(0.0)$ on $\partial\Omega$. Then the bending stiffness is belonging to Sturm-Liouville class, $\mathsf{A}\in SL(\Omega)$, under the inner-product of (1). The proof follows.

Let two operators P and Q be defined by $\mathrm{P} = \rho^{-1}\nabla^2$ and $\mathsf{Q} = k\nabla^2$, then the bending stiffness A becomes their composite, i.e. $\mathrm{A} = \mathrm{PQ}$. For any $\psi, \phi \in D(\mathsf{A})$,

$$\langle \mathsf{PQ}\psi, \phi \rangle_\Omega = \langle \mathsf{Q}\psi, \mathsf{P}\phi \rangle_\Omega,$$

since $\alpha_1(\mathsf{Q}\psi) + \beta_1\nabla(\mathsf{Q}\psi)\cdot\hat{n} = 0$ and $\alpha_1\phi + \beta_1\nabla\phi\cdot\hat{n} = 0$. Moreover,

$$\langle \psi, \mathsf{PQ}\phi \rangle_\Omega = \langle \mathsf{P}\psi, \mathsf{Q}\phi \rangle_\Omega,$$

Since $\alpha_2(\mathsf{Q}\phi) + \beta_2\nabla(\mathsf{Q}\phi)\cdot\hat{n} = 0$; $\alpha_2\psi + \beta_2\nabla\psi\cdot\hat{n} = 0$. Observe that

$$\langle \mathsf{P}\psi, \mathsf{Q}\phi \rangle_\Omega = \langle \mathsf{Q}\psi, \mathsf{P}\phi \rangle_\Omega,$$

since both sides equal $\int_\Omega k\nabla^2\psi\cdot\nabla^2\phi\, dV$. Therefore, the bending stiffness operator A is self-adjoint. Moreover, the inverse of A is a compact operator in $L_2(\Omega)$, since A is fourth-order differential operator. Therefore, its eigenfunctions constitute a real, orthonormal, and complete basis of $L_2(\Omega)$ under the inner-product of (1).

3. 2D Transfer Function- a New Tool

With respect to the eigenfunctions set $\{\phi_\lambda\}_{\lambda\in\Lambda}$ of a Sturm-Liouville operator A, the Galerkin transform G from spatial functions to modal functions, $F(\lambda) = \mathsf{G}[f(x)]$, is defined by

$$F(\lambda) \equiv \int_\Omega \rho(x)\phi_\lambda(x) f(x)\, dx. \tag{2}$$

Completeness and orthonormality of $\{\phi_\lambda\}_{\lambda\in\Lambda}$ of countable cardinality jointly imply that the Galerkin transform G has a unique inverse G^{-1}, $\mathrm{f(x)} = \mathrm{G}^{-1}[\mathrm{F}(\lambda)]$:

$$f(x) \equiv \sum_{\lambda\in\Lambda} F(\lambda)\phi_\lambda(x). \tag{3}$$

Then, Laplace-Galerkin transform H from spatial-temporal functions to modal-complex functions is defined by the composite of Galerkin transform G and Laplace transform L:

$$\mathsf{H} = \mathsf{LG} = \mathsf{GL};$$

explicitly,

$$F(\lambda, s) \equiv \mathsf{H}[f(x,t)] = \int_{0^-}^{\infty}\int_\Omega e^{-st}\rho(x)\phi_\lambda(x) f(x,t)\, dx dt. \tag{4}$$

Accordingly, the inverse of Laplace-Galerkin transform H^{-1} is the composite of the inverse of Laplace transform and that of Galerkin transform, that is,

$$\mathsf{H}^{-1} = \mathsf{G}^{-1}\mathsf{L}^{-1} = \mathsf{L}^{-1}\mathsf{G}^{-1};$$

explicitly,

$$f(x,t) \equiv \mathsf{H}^{-1}[F(\lambda,s)] = \frac{1}{2\pi j}\sum_{\lambda\in\Lambda}\int_\Gamma F(\lambda,s)\phi_\lambda(x) e^{ts}\, ds. \tag{5}$$

Here the domain Γ is an infinite line parallel to the imaginary axis, whereon the integral in (4) is converged.

Denote the temporal derivative $\partial/\partial t$ by D_t, and let A be a Sturm-Liouville operator, $\mathsf{A}\in SL(\Omega)$. Especially for boundary and initial homogeneity, there are two basic properties about Galerkin and Laplace transforms:

$$\mathsf{G}[\mathsf{A}f(x,t)] = \lambda\mathsf{G}[f(x,t)] \tag{6}$$

based on Green's identity, and

$$\mathsf{L}[\mathsf{D}_t f(x,t)] = s\mathsf{L}[f(x,t)]. \tag{7}$$

Moreover, for any parabolic or hyperbolic dynamics $\hat{G}$, its spatiotemporal impulse response of $\hat{G}$ is defined by

$$g(x,t) = \mathsf{H}^{-1}[G(\lambda,s)] \tag{8}$$

As an explanatory example of 2D transfer-function, let us find the impulse response of the following wave equation $\hat{G}$:

$$\frac{\partial^2\psi}{\partial t^2} - \frac{\partial^2\psi}{\partial x^2} = u,\ 0\le x\le\pi,\ 0\le t<\infty;$$

$$\psi(0,t) = 0,\ \psi(\pi,t) = 0,\ 0\le t<\infty.$$

$$\psi(x,0) = 0,\ \dot{\psi}(x,0) = 0,\ 0\le x\le\pi.$$

The elastic stiffness $-\partial^2/\partial x^2$ is of eigenvalues

$$\Lambda = \{1,4,9,\cdots\}$$

associated with eigenfunctions $\phi_\lambda(x)=\sqrt{2/\pi}\sin\sqrt{\lambda}x$. Taking the Laplace-Galerkin transform H on both sides of the differential equation yields

$$(s^2+\lambda)\Psi(\lambda,s)=U(\lambda,s),$$

that is, the 2D transfer-function of the dynamics $\hat{G}$ is

$$G(\lambda,s)\equiv\frac{\Psi(\lambda,s)}{U(\lambda,s)}=\frac{1}{s^2+\lambda}.$$

Correspondingly, the impulse response $g=\mathsf{H}^{-1}G$ is

$$g(x,t)=\sum_{\omega=1}^{\infty}\sqrt{2/\pi}\sin\omega x\cdot\mathsf{L}^{-1}\left(\frac{1}{s^2+\omega^2}\right)=\sum_{\omega=1}^{\infty}\frac{\sqrt{2}}{\omega\sqrt{\pi}}\sin\omega x\sin\omega t.$$

To check whether this solution is correct, let us give the dynamics $\hat{G}$ the 2D unit-pulse $u(x,t)=\delta(t)\sum_{\lambda\in\Lambda}\phi_\lambda(x)$, where $\mathsf{H}u=1$. Integration of the differential equation from $t=0^-$ to $t=0^+$ yields the initial condition: $\psi(x,0)=0$ and $\dot{\psi}(x,0)=\sum_{\lambda\in\Lambda}\phi_\lambda(x)$. Thereby, the impulse response g is just the solution of the initial-value problem:

$$\frac{\partial^2\psi}{\partial t^2}-\frac{\partial^2\psi}{\partial x^2}=0,$$

$$\psi(0,t)=0,\ \psi(\pi,t)=0,$$

$$\psi(x,0)=0,\ \dot{\psi}(x,0)=\sum_{\lambda\in\Lambda}\phi_\lambda(x),$$

which has the form solvable by the conventional Separation-of-Variables method. It can be found that two solutions are identical. Therefore, representation of Sturm-Liouville dynamics by 2D transfer-functions captures the memory nature of dynamics, and therefore results in unconfused dynamic responses driven by spatial-temporally impulsive or discontinuous inputs.

4. Virtual-Source Conversion of Boundary Inhomogeneity

By a series of examples, this section demonstrates how to converts the boundary or initial inhomogeneity into virtual source in conjunction with boundary or initial homogeneity.

For the first example, consider the acoustic dynamics $\hat{G}$:

$$\frac{\partial^2\psi}{\partial t^2}-\frac{\partial^2\psi}{\partial x^2}=0,\ \psi(0,t)=0,\ \psi(\pi,t)=0,$$

with inhomogeneous boundary conditions:

$$\psi(x,0)=0,\ \dot{\psi}(x,0)=f(x).$$

With integration by parts, taking the Laplace-Galerkin transform H on the differential equation yields

$$\Psi(\lambda,s)=\frac{1}{s^2+\lambda}\mathsf{G}[f(x)].$$

Taking the inverse Laplace-Galerkin transform H^{-1} on the above equation yields

$$\frac{\partial^2\psi}{\partial t^2}-\frac{\partial^2\psi}{\partial x^2}=f(x)\delta(t),\ \psi(0,t)=0,\ \psi(\pi,t)=0,$$

$$\psi(x,0)=0,\ \dot{\psi}(x,0)=0,$$

where δ is the Dirac delta distribution. That is, these two PDE models point to the same response for $t\ge 0^+$.

For the second example, consider the following thermoacoustic vibration $\hat{G}$:

$$\frac{\partial^2\psi}{\partial t^2}-\frac{1}{\rho}\nabla\cdot(k\nabla\psi)=0\ \text{ in }\ \Omega, \tag{9}$$

$$\alpha\psi+\beta\nabla\psi\cdot\hat{n}=f\ \text{ on }\ \partial\Omega, \tag{10}$$

where $\rho(x)>0$, $k(x)>0$ for $\forall x\in\Omega$, and $\alpha(x)$, $\beta(x)$ are real $\forall x\in\partial\Omega$ but not both zero. This dynamics involves the elastic stiffness A:

$$\mathsf{A}\phi=-(1/\rho)\nabla\cdot(k\nabla\phi)\ \text{ in }\ \Omega,$$

$$\alpha\phi+\beta\nabla\phi\cdot\hat{n}=0\ \text{ on }\ \partial\Omega.$$

As shown in Section 2, the elastic stiffness A is a Sturm-Liouville operator $\mathsf{A}\in SL(\Omega)$ under the inner-product of (1). Let $\Phi=\{\phi_\lambda\}_{\lambda\in\Lambda}$ denote the eigenfunctions set of A corresponding to the eigenvalues set Λ.

On the boundary $\partial\Omega$, firstly, substitution $\alpha\phi_\lambda+\beta\nabla\phi_\lambda\cdot\hat{n}=0$ for $(10)\times(-\phi_\lambda)$ yields

$$(\psi\nabla\phi_\lambda-\phi_\lambda\nabla\psi)\cdot\hat{n}=(-\phi_\lambda/\beta)f\ \text{ for }\ \beta\neq 0.$$

Secondly, substitution of

$$\alpha\phi_\lambda+\beta\nabla\phi_\lambda\cdot\hat{n}=0$$

for $(10)\times\nabla\phi_\lambda\cdot\hat{n}$ yields

$$(\psi\nabla\phi_\lambda-\phi_\lambda\nabla\psi)\cdot\hat{n}=(\nabla\phi_\lambda\cdot\hat{n}/\alpha)f\ \text{ for }\ \alpha\neq 0.$$

In general, the sum of the first equation$\times\beta/(\alpha+\beta)$ and the second equation$\times\alpha/(\alpha+\beta)$ becomes

$$(\psi\nabla\phi_\lambda-\phi_\lambda\nabla\psi)\cdot\hat{n}=\frac{(-\phi_\lambda+\nabla\phi_\lambda\cdot\hat{n})}{\alpha+\beta}f.$$

Moreover, based on the Green's identity,

$$\begin{aligned}&\int_\Omega \phi_\lambda \nabla\cdot(k\nabla\psi)\,dV\\&=\int_\Omega \psi\nabla\cdot(k\nabla\phi_\lambda)\,dV+\oint_{\partial\Omega} k(\psi\nabla\phi_\lambda-\phi_\lambda\nabla\psi)\cdot\hat{n}dS\end{aligned}.$$

With these formulas, performing Laplace-Galerkin transform on (9) yields

$$\begin{aligned}(s^2+\lambda)\Psi(\lambda,s)&=\oint_{\partial\Omega} k(\phi_\lambda\nabla\psi-\psi\nabla\phi_\lambda)\cdot\hat{n}dS\\&\equiv\oint_{\partial\Omega} k(x)B_\lambda(x)\hat{f}(x,s)\,dS\equiv Q(\lambda,s)\end{aligned},$$

where $\Psi(\lambda,s)\equiv \mathsf{H}[\psi(x,t)]$, $\hat{f}(x,s)\equiv \mathsf{L}[f(x,t)]$, and B_λ equals

$$\begin{cases}\dfrac{\phi_\lambda}{\beta}, \text{for } \beta\neq 0\\ \dfrac{-\nabla\phi_\lambda\cdot\hat{n}}{\alpha}, \text{for } \alpha\neq 0\\ \dfrac{\phi_\lambda-\nabla\phi_\lambda\cdot\hat{n}}{\alpha+\beta}, \text{in general}\end{cases}.$$

Therefore, the 2D transfer-function G of the dynamics $\hat{G}$ in (9)-(10) is

$$G(\lambda,s)\equiv\frac{\Psi(\lambda,s)}{Q(\lambda,s)}=\frac{1}{s^2+\lambda},$$

Performing the inverse Laplace-Galerkin transform H^{-1} on the above equation yields

$$\frac{\partial^2\psi}{\partial t^2}-\frac{1}{\rho}\nabla\cdot(k\nabla\psi)=q \quad\text{in } \Omega, \tag{11}$$

$$\alpha\psi+\beta\nabla\psi\cdot\hat{n}=f \quad\text{on } \partial\Omega, \tag{12}$$

where $q(x,t)\equiv \mathsf{H}^{-1}[Q(\lambda,s)]$.

That is, in the interior of the domain Ω, the response governed by (9)-(10) is identical to that governed by (11)-(12), since both have the same 2D transfer-function.

For the third example, consider the following beam vibration $\hat{G}$:

$$\frac{\partial^2\psi}{\partial t^2}+\frac{1}{\rho}\frac{\partial^2}{\partial x^2}(k\frac{\partial^2\psi}{\partial x^2})=0 \quad\text{in } [0,\ell], \tag{13}$$

$$\alpha_1(k\psi'')+\beta_1(k\psi'')'=f_1,\ \ \alpha_2\psi+\beta_2\psi'=f_2 \quad\text{at } x=0, \tag{14}$$

$$\psi=0 \ \text{ and } \ \psi''=0 \quad\text{at } x=\ell, \tag{15}$$

where $\rho(x)>0$, $k(x)>0$ for all $x\in[0,\ell]$, $\beta_1\neq 0$, and $\beta_2\neq 0$. This dynamics involves the bending stiffness A in Section 2:

$$\mathsf{A}\phi=\frac{1}{\rho}\frac{\partial^2}{\partial x^2}(k\frac{\partial^2\phi}{\partial x^2}) \quad\text{in } [0,\ell],$$

$$\alpha_1\phi+\beta_1\phi'=0 \ \text{ and } \ \alpha_2(k\phi'')+\beta_2(k\phi'')'=0 \quad\text{at } x=0,$$

$$\phi=0 \ \text{ and } \ \phi''=0 \quad\text{at } x=\ell, \tag{16}$$

which is a Sturm-Liouville operator, $\mathsf{A}\in SL([0,\ell])$, under the inner-product of (1). Let us denote its eigenvalues set by Λ and eigenfunctions set by $\Phi=\{\phi_\lambda\}_{\lambda\in\Lambda}$.

With integration by parts (one-dimensional Green's identity),

$$\begin{aligned}&\int_0^\ell \phi_\lambda(k\psi'')''dx=\int_0^\ell \psi(k\phi_\lambda'')''dx\\&+\left(\phi_\lambda'(k\psi'')-\phi_\lambda(k\psi'')'+\psi(k\phi_\lambda'')'-\psi'(k\phi_\lambda'')\right)\Big|_{x=0}\end{aligned}.$$

By substituting (16) into (14), this equation becomes

$$\int_0^\ell \phi_\lambda(k\psi'')''dx=\int_0^\ell \psi(k\phi_\lambda'')''dx-\frac{\phi_\lambda(0)}{\beta_1}f_1-\frac{k(0)\phi_\lambda''(0)}{\beta_2}f_2.$$

Thus, performing the Laplace-Galerkin transform H on (13) yields

$$(s^2+\lambda)\Psi(\lambda,s)=\frac{\phi_\lambda(0)}{\beta_1}F_1(s)+\frac{k(0)\phi_\lambda''(0)}{\beta_2}F_2(s).$$

Performing the inverse Laplace-Galerkin transform H^{-1} on the above equation yields

$$\begin{aligned}&\frac{\partial^2\psi}{\partial t^2}+\frac{1}{\rho}\frac{\partial^2}{\partial x^2}(k\frac{\partial^2\psi}{\partial x^2})\\&=\frac{1}{\beta_1\rho(0)}f_1(t)\delta(x)+\frac{k(0)}{\beta_2}f_2(t)\sum_{\lambda\in\Lambda}\phi_\lambda''(0)\phi_\lambda(x)\end{aligned}, \tag{17}$$

$$\alpha_1(k\psi'')+\beta_1(k\psi'')'=0 \ \text{ and } \ \alpha_2\psi+\beta_2\psi'=0 \quad\text{at } x=0,$$

$$\psi=0 \ \text{ and } \ \psi''=0 \quad\text{at } x=\ell,$$

where the last term of the right-hand side in (17) includes the second derivative of the Delta function $\delta''(x)$. This response is identical to that of (13)-(15) in $(0,\ell]$, since they have the identical transfer-function.

The above examples show how the parabolic or hyperbolic dynamics with inhomogeneous boundary/initial condition can be converted to impulsive source on boundary in conjunction with boundary/initial homogeneity.

5. Numerical Visualization

In this section, conventional and virtual-source solutions of a simple heat-condition with one-side Dirichlet inhomogeneity is computed and then visualized in figures. It is expected to visualize between them the identical parts in the interior but the topological difference on the inhomogeneous boundary. Accordingly, consider the solution of the following parabolic dynamics:

$$\frac{\partial y}{\partial t}-\frac{\partial^2 y}{\partial x^2}=0\text{, for } x\in[0,\pi],\ t\in[0,\infty);$$

$$y(0,t)=f(t);\ y(\pi,t)=0\text{; for } t\in[0,\infty);$$

$$y(x,0)=0 \text{ for } x\in[0,\pi].$$

Two cases of environments are considered: one is time-invariant in which $f(t)=1$, and the other is time-varying in which $f(t)=\sin\omega t$.

The conventional approach is firstly applied to solve the Case I. Thereby, let the temperature distribution y be decomposed into

$$y(x,t)=\bar{y}(x)+\psi(x,t),$$

Where the steady-state solution $\bar{y}$ is governed by

$$\frac{d^2\bar{y}}{dx^2}=0,\ \bar{y}(0)=1,\ \bar{y}(\pi)=0;$$

and the transient solution ψ is governed by

$$\frac{\partial\psi}{\partial t}-\frac{\partial^2\psi}{\partial x^2}=0,\ \psi(0,t)=0,\ \psi(\pi,t)=0,\ \psi(x,0)=-\bar{y}(x).$$

Therein the transient equation is of boundary homogeneity, so it can be solved by the method of separation-of-variables. In this method,

$$\psi(x,t)=\sum_{n=1}^{\infty}\eta_n(t)\phi_n(x),$$

where $\phi_n(x)=\sqrt{2/\pi}\sin nx$, and

$$\dot{\eta}_n+n^2\eta_n=0,$$

$$\eta_n(0)=\langle-\bar{y},\phi_n\rangle=\sqrt{\frac{2}{\pi}}\frac{1}{n}\left[(-1)^{n+1}+(-1)^n-1\right].$$

That is,

$$y(x,t)=\frac{-1}{\pi}x+1+\frac{2}{\pi}\sum_{n=1}^{N}\frac{b_n}{n}\sin nx\cdot e^{-n^2t},$$

$$b_n\equiv(-1)^{n+1}+(-1)^n-1. \tag{18}$$

In fact, the transient solution ψ can also be solved by the virtual-source realization of initial inhomogeneity as shown in the first example of Section 4. Therein, with the approach the 2D transfer-function, the transient equation is realized by virtual source as

$$\frac{\partial\psi}{\partial t}-\frac{\partial^2\psi}{\partial x^2}=-\bar{y}(x)\delta(t),$$

$$\psi(0,t)=0,\ \psi(\pi,t)=0,\ \psi(x,0)=0,$$

which is boundary and initial homogeneity. Taking the Laplace-Galerkin transform on this equations yields

$$\Psi(\lambda,s)=\frac{1}{s+n^2}\frac{b_n}{n}\sqrt{\frac{2}{\pi}}\ (n=\sqrt{\lambda}).$$

Taking the inverse Laplace-Galerkin transform on Ψ yields the identical solution:

$$\psi(x,t)=\frac{2}{\pi}\sum_{n=1}^{N}\frac{b_n}{n}\sin nx\cdot e^{-n^2t}.$$

Secondly, the virtual-source realization, as shown in Section 4, is employed to solve the Case I and Case II. Based on the Green's identity,

$$\langle y'',\phi_n\rangle=-y\phi_n'\Big|_0^{\pi}+\langle y,\phi_n''\rangle. \tag{19}$$

Taking the Laplace-Galerkin transform on the heat-conduction dynamics above yields

$$Y(n,s)=\phi_n'(0)\cdot\frac{F(s)}{s+n^2}. \tag{20}$$

As $f(t)=1$, $F(s)=1/s$. Then taking the inverse Laplace-Galerkin transform on Y yields

$$y(x,t)=\frac{2}{\pi}\sum_{n=1}^{N}\sin nx\cdot\frac{1}{n}(1-e^{-n^2t}) \tag{21}$$

In case II, let $f(t)$ be $\sin\omega t$ and then $F(s)=\omega/(s^2+\omega^2)$. By the similar procedure,

$$y(x,t)=\frac{2}{\pi}\sum_{n=1}^{N}\frac{n}{n^4+\omega^2}\sin nx\cdot(\omega e^{-n^2t}+n^2\sin\omega t-\omega\cos\omega t) \tag{22}$$

However, the separation-of-variables method is improper to be employed to solve the solution of Case II, wherein the environmental temperature is time-varying.

Figure 1 shows the order-reduced solutions of Case I with 300 modes being considered, wherein at $t=0.8$ the separation-of-variable solution of (18) is in juxtaposition with the virtual-source solution of (21) for comparison. It is bound that both solutions are identical in the interior of the domain, as predicted. However, close view on the inhomogeneous boundary $x=0$ as shown in Figure 2 reveals that the exact solution ($N\to\infty$) by the virtual-source realization is discontinuous at $x=0$. In fact, this has been suggested by (20) above. With the inverse Laplace-Galerkin transform, (20) is equivalent to

$$\frac{\partial y}{\partial t}-\frac{\partial^2 y}{\partial x^2}=-\delta'(x)f(t)\,, \tag{23}$$

with boundary and initial homogeneity. Equation (23) implies that the virtual source is actually impulsive on the inhomogeneous boundary, which converts the boundary/initial conditions into delta sources and/or their derivatives.

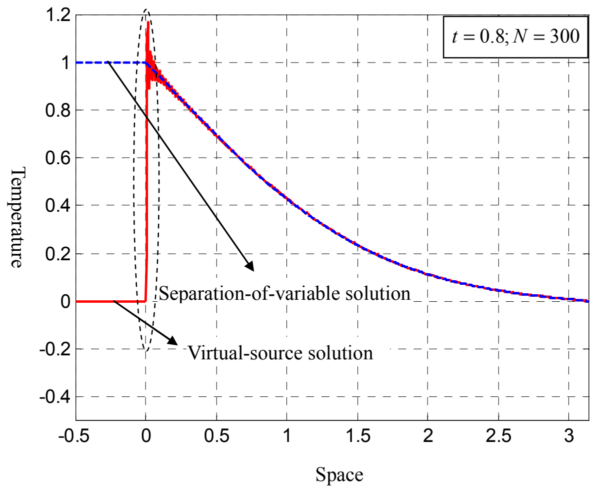

Figure 1. *Topological comparison of the virtual-source solution with the separation-of-variables solution under time-invariant environment*

Figures 3 and 4 shows the virtual-source solution under time-varying environment: $f(t)=\sin t$. At $t=0.8$, two order-reduced solutions according to $N=200$ and $N=1000$, respectively, are juxtaposed with each other. The situation of converging implies that the solution will reach discontinuity at $x=0$ as $N\to\infty$. This verifies again that the virtual-source strategy is zeroing the environment and simultaneously giving impulsive source on the inhomogeneous boundary.

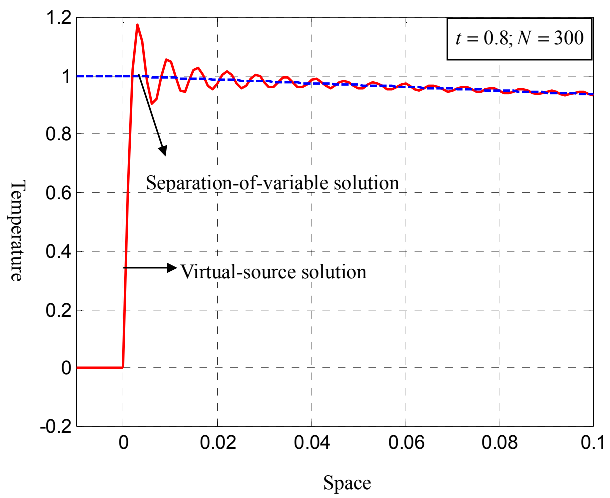

Figure 2. *Close view of Figure 1*

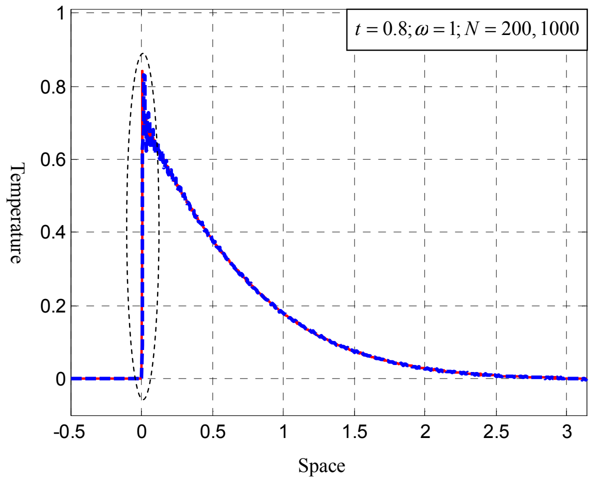

Figure 3. *Topological convergence of the virtual-source solution under time-varying environment*

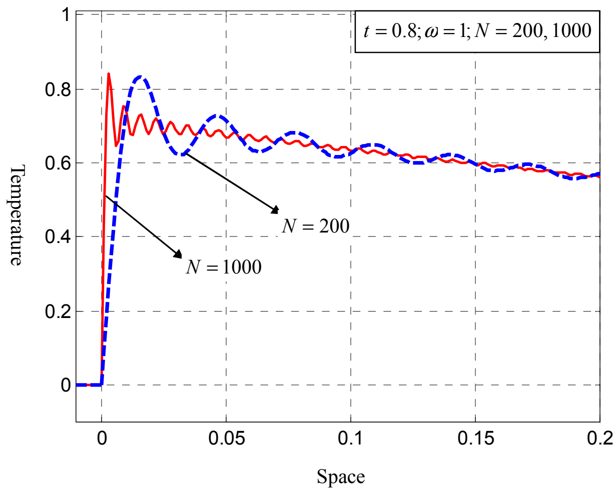

Figure 4. *Close view of Figure 3*

6. Summary

This paper provides the virtual-source realization to cleverly solve parabolic and hyperbolic dynamics with inhomogeneous boundary conditions. It is especially for modal decomposition under time-varying environments and Robin inhomogeneity, which is beyond conventional approaches. It is found that the virtual source is actually impulsive on the inhomogeneous boundary, which converts the boundary conditions into delta sources and/or their derivatives. Its strategy is to zero the environment and simultaneously to create an impulsive source on the inhomogeneous boundary. These findings are obtained through the Hilbert space in which the 2D transfer function and Laplace-Galerkin transform are constructed as the main tools for this work.

Acknowledgements

Thank the Ministry of Science and Technology of Taiwan for financially supporting this work with the project grant: 103 - 2221 - E - 194 - 041.

References

[1] B.-S. Hong, "Construction of 2D isomorphism for 2D H_∞-control of Sturm-Liouville Systems," Asian J. Control, vol. 12, no. 2, pp. 187-199, 2010.

[2] B.-S. Hong and C.-Y. Chou, "Realization of thermal inertia in frequency domain," Entropy, vol. 16, pp. 1101-1121, 2014.

[3] B.-S. Hong and C.-Y. Chou, "Energy transfer modelling of active thermoacoustic engines via Lagrangian thermoacoustic dynamics," Energy Convers. Manage., vol. 84, pp. 73-79, 2014.

[4] B.-S. Hong, V. Yang, and A. Ray, "Robust feedback control of combustion instability with modeling uncertainty," Combust. Flame, vol. 120, pp. 91-106, 2000.

[5] B.-S. Hong, A. Ray, and V. Yang, "Wide-range robust control of combustion instability," Combust. Flame, vol. 128, pp. 242-258, 2002.

[6] K. Gustafson and T. Abe, "Gustave Robin: 1855–1897," Math. Intelligencer, vol. 20, pp. 47–53, 1998.

[7] K. Gustafson and T. Abe, "The third boundary condition—was it Robin's?," Math. Intelligencer, vol. 20, no. 1, pp. 63–71, 1998.

[8] A. Romeo and A. A Saharian, "Casimir effect for scalar fields under Robin boundary conditions on plates," J. Phys. A: Math. Gen,. vol. 35, p. 1297, 2002.

[9] B. Mintz, C. Farina, P. A. Maia Neto, and R. B. Rodrigues, "Particle creation by a moving boundary with a Robin boundary condition," J. Phys. A: Math. Gen. vol. 39, pp. 11325–11333, 2006.

[10] E. Okada, M. Schweiger, S. R. Arridge, M. Firbank, and D. T. Delpy, "Experimental validation of Monte Carlo and finite-element methods for the estimation of the optical path length in inhomogeneous tissue," Applied Optics, vol. 35, no. 19, pp. 3362-3371, 1996.

[11] F. Bay, V. Labbe, Y. Favennec, and J. L. Chenot, "A numerical model for induction heating processes coupling electromagnetism and thermomechanics," Int. J. Numer. Meth. Engng, vol. 58, pp. 839–867, 2003.

[12] B. Jin, "Conjugate gradient method for the Robin inverse problem, associated with the Laplace equation," Int. J. Numer. Meth. Engng, vol. 71, pp. 433–453, 2007.

[13] X. T. Xiong, X. H. Liu, Y. M. Yan, and H. B. Guo, "A numerical method for identifying heat transfer coefficient," Appl. Math. Model, vol. 34, pp. 1930–1938, 2010.

[14] E. Majchrzak and M. Paruch, "Identification of electromagnetic field parameters assuring the cancer destruction during hyperthermia treatment," Inverse Probl. Sci. Eng., vol. 19, no. 1, pp. 45-58, 2011.

[15] B. Jin and X. Lu, "Numerical identification of a Robin coefficient in parabolic problems," Math. Comp., vol. 81, pp. 1369-1398, 2012.

[16] A. Moosaie, "Axisymmetric non-Fourier temperature field in a hollow sphere," Arch. Appl. Mech., vol. 79, pp. 679-694 2009.

[17] B. Abdel-Hamid, "Modelling non-Fourier heat conduction with periodic thermal oscillation using the finite integral transform," Appl. Math. Model. vol. 23, pp. 899–914, 1999.

[18] G. Heidarinejad, R. Shirmohammadi, and M. Maerefat, "Heat wave phenomena in solids subjected to time dependent surface heat flux," Heat Mass Transf., vol. 44, pp. 381–392, 2008.

[19] N. Young, An Introduction to Hilbert Space. Cambridge University Press, 1988.